

Scattering of Dirac Waves off Kerr Black Holes

S. K. Chakrabarti and Banibrata Mukhopadhyay

S.N. Bose National Centre for Basic Sciences,

JD-Block, Sector III, Salt Lake, Calcutta 700091, India

chakraba@boson.bose.res.in and bm@boson.bose.res.in

Accepted for publication in MNRAS

ABSTRACT

Chandrasekhar separated the Dirac equation for spinning and massive particles in Kerr geometry into radial and angular parts. Here we solve the complete wave equation and find out how the Dirac wave scatters off Kerr black holes. The eigenfunctions, eigenvalues and reflection and transmission co-efficients are computed. We compare the solutions with several parameters to show how a spinning black hole distinguishes mass and energy of incoming waves. Very close to the horizon the solutions become independent of the particle parameters indicating an universality of the behaviour.

Key words: Black holes – spin-1/2 particles – Dirac equations – Waves: scattering

1 INTRODUCTION

Chandrasekhar (1976) separated Dirac equation in Kerr black hole geometry into radial (r) and angular (θ) parts. The radial equations governing the radial wave-functions $R_{\pm\frac{1}{2}}$ corresponding to spin $\pm\frac{1}{2}$ are given by (with $\hbar = 1 = G = c$):

$$\Delta^{\frac{1}{2}}\mathcal{D}_0R_{-\frac{1}{2}} = (\lambda + im_p r)\Delta^{\frac{1}{2}}R_{+\frac{1}{2}}; \quad \Delta^{\frac{1}{2}}\mathcal{D}_0^\dagger\Delta^{\frac{1}{2}}R_{+\frac{1}{2}} = (\lambda - im_p r)R_{-\frac{1}{2}}, \quad (1)$$

where, the operators \mathcal{D}_n and \mathcal{D}_n^\dagger are given by,

$$\mathcal{D}_n = \partial_r + \frac{iK}{\Delta} + 2n\frac{(r-M)}{\Delta}; \quad \mathcal{D}_n^\dagger = \partial_r - \frac{iK}{\Delta} + 2n\frac{(r-M)}{\Delta}, \quad (2)$$

and

$$\Delta = r^2 + a^2 - 2Mr; \quad K = (r^2 + a^2)\sigma + am. \quad (3)$$

Here, a is the Kerr parameter, n is an integer, σ is the frequency of incident wave, M is the mass of the black hole, m_p is the rest mass of the Dirac particle, λ is the eigenvalue which is the separation constant of complete Dirac equation and m is the azimuthal quantum number.

The equations governing the angular wave-functions $S_{\pm\frac{1}{2}}$ corresponding to spin $\pm\frac{1}{2}$ are given by:

$$\mathcal{L}_{\frac{1}{2}}S_{+\frac{1}{2}} = -(\lambda - am_p \cos \theta)S_{-\frac{1}{2}}; \quad \mathcal{L}_{\frac{1}{2}}^\dagger S_{-\frac{1}{2}} = +(\lambda + am_p \cos \theta)S_{+\frac{1}{2}} \quad (4)$$

where, the operators \mathcal{L}_n and \mathcal{L}_n^\dagger are given by,

$$\mathcal{L}_n = \partial_\theta + Q + n \cot \theta; \quad \mathcal{L}_n^\dagger = \partial_\theta - Q + n \cot \theta \quad (5)$$

and

$$Q = a\sigma \sin \theta + m \operatorname{cosec} \theta. \quad (6)$$

Combining eqs. 4, one obtains a second order angular eigenvalue equations which admits exact solutions for spin-half particles when $\rho = \frac{m_p}{\sigma} = 1$ (Chakrabarti, 1984),

$$\lambda^2 = \left(l + \frac{1}{2}\right)^2 + a\sigma(p + 2m) + a^2\sigma^2 \left[1 - \frac{y^2}{2(l+1) + a\sigma x}\right], \quad (7)$$

and

$$\frac{1}{2}S_{lm} = \frac{1}{2}Y_{lm} - \frac{a\sigma y}{2(l+1) + a\sigma x} \frac{1}{2}Y_{l+1m} \quad (8)$$

where,

$$p = F(l, l); \quad x = F(l+1, l+1); \quad y = F(l, l+1)$$

and

$$F(l_1, l_2) = [(2l_2+1)(2l_1+1)]^{\frac{1}{2}} \langle l_2 1 m 0 | l_1 m \rangle \left[\langle l_2 1 \frac{1}{2} 0 | l_1 \frac{1}{2} \rangle + (-1)^{l_2-l} \langle l_2 1 m 0 | l_1 m \rangle \right. \\ \left. + \langle l_2 1 \frac{1}{2} 0 | l_1 \frac{1}{2} \rangle + (-1)^{l_2-l} \rho \sqrt{2} \langle l_2 1 - \frac{1}{2} 1 | l_1 \frac{1}{2} \rangle \right]. \quad (9)$$

Here, $\langle \dots | \dots \rangle$ are the usual Clebsh-Gordon coefficients and ${}_s Y_{lm}$ are the standard spin-weighted spherical harmonics (Chakrabarti, 1984; see also, Goldberg et al 1967, Breure et al, 1982) of spin s and usual quantum numbers l and m . When $\rho \neq \frac{m_p}{\sigma} = 1$, one obtains the

solutions perturbatively with $a\sigma$ to be the perturbation parameter. The detailed procedure to obtain eigenfunctions and eigenvalues is in (Chakrabarti 1984) and is not described here.

The radial equations (1) are in coupled form. One can decouple them and express the equation either in terms of spin up or spin down wave functions $R_{\pm\frac{1}{2}}$ but the expression loses its transparency. It is thus advisable to use the approach of Chandrasekhar (1983) by changing the basis and independent variable r to,

$$r_* = r + \frac{2Mr_+ + am/\sigma}{r_+ - r_-} \log\left(\frac{r}{r_+} - 1\right) - \frac{2Mr_- + am/\sigma}{r_+ - r_-} \log\left(\frac{r}{r_-} - 1\right) \quad (r > r_+). \quad (10)$$

where,

$$\frac{d}{dr_*} = \frac{\Delta}{\omega^2} \frac{d}{dr}; \quad \omega^2 = r^2 + \alpha^2; \quad \alpha^2 = a^2 + am/\sigma, \quad (11)$$

to transform the set of coupled equations (eq. 1) into two independent one dimensional wave equations given by:

$$\left(\frac{d}{dr_*} - i\sigma\right) P_{+\frac{1}{2}} = \frac{\Delta^{\frac{1}{2}}}{\omega^2} (\lambda - im_p r) P_{-\frac{1}{2}}; \quad \left(\frac{d}{dr_*} + i\sigma\right) P_{-\frac{1}{2}} = \frac{\Delta^{\frac{1}{2}}}{\omega^2} (\lambda + im_p r) P_{+\frac{1}{2}}. \quad (12)$$

Here, $\mathcal{D}_0 = \frac{\omega^2}{\Delta} (\frac{d}{dr_*} + i\sigma)$ and $\mathcal{D}_0^\dagger = \frac{\omega^2}{\Delta} (\frac{d}{dr_*} - i\sigma)$ were used and wave functions were redefined as $R_{-\frac{1}{2}} = P_{-\frac{1}{2}}$ and $\Delta^{\frac{1}{2}} R_{+\frac{1}{2}} = P_{+\frac{1}{2}}$.

2 SOLUTION PROCEDURE

We define a new variable,

$$\theta = \tan^{-1}(m_p r / \lambda), \quad \text{which gives,} \quad (\lambda \pm im_p r) = \exp(\pm i\theta) \sqrt{(\lambda^2 + m_p^2 r^2)}. \quad (13)$$

Also define,

$$P_{+\frac{1}{2}} = \psi_{+\frac{1}{2}} \exp\left[-\frac{1}{2}i \tan^{-1}\left(\frac{m_p r}{\lambda}\right)\right]; \quad P_{-\frac{1}{2}} = \psi_{-\frac{1}{2}} \exp\left[+\frac{1}{2}i \tan^{-1}\left(\frac{m_p r}{\lambda}\right)\right], \quad (14)$$

and further choosing $\hat{r}_* = r_* + \frac{1}{2\sigma} \tan^{-1}\left(\frac{m_p r}{\lambda}\right)$ so that $d\hat{r}_* = \left(1 + \frac{\Delta}{\omega^2} \frac{\lambda m_p}{2\sigma} \frac{1}{\lambda^2 + m_p^2 r^2}\right) dr_*$, and $Z_{\pm} = \psi_{+\frac{1}{2}} \pm \psi_{-\frac{1}{2}}$ the above equations become,

$$\left(\frac{d}{d\hat{r}_*} - W\right) Z_+ = i\sigma Z_-; \quad \left(\frac{d}{d\hat{r}_*} + W\right) Z_- = i\sigma Z_+, \quad (15)$$

where,

$$W = \frac{\Delta^{\frac{1}{2}} (\lambda^2 + m_p^2 r^2)^{3/2}}{\omega^2 (\lambda^2 + m_p^2 r^2) + \lambda m_p \Delta / 2\sigma}. \quad (16)$$

From these equations, we readily obtain a pair of independent one-dimensional wave equations,

$$\left(\frac{d^2}{d\hat{r}_*^2} + \sigma^2\right) Z_{\pm} = V_{\pm} Z_{\pm}; \quad \text{where} \quad V_{\pm} = W^2 \pm \frac{dW}{d\hat{r}_*}. \quad (17)$$

By transformation of the variable from r to r_* (and \hat{r}_*) the horizon is shifted from $r = r_+$ to $\hat{r}_* = -\infty$ unless $\sigma \leq \sigma_s = -am/2Mr_+$ (eq. 10). In this connection, it is customary to define σ_c where $\alpha^2 = 0$ (eq. 11). Thus, $\sigma_c = -m/a$. If $\sigma \leq \sigma_s$, super-radiation is expected for particles with integral spins but not for those with half-integral spin (Chandrasekhar 1983). Thus, we concentrate on the region where, $\sigma > \sigma_s$.

The choice of parameters is generally made in such a way that there is a significant interaction between the particle and the black hole, i.e., when the Compton wavelength of the incoming wave is of the same order as the outer horizon of the Kerr black hole. Similarly, the frequency of the incoming particle (or wave) should be of the same order as inverse of light crossing time of the radius of the black hole. These yield,

$$m_p \sim \sigma \sim [M + \sqrt{(M^2 - a^2)}]^{-1}. \quad (18)$$

Thus, we need to deal with quantum black holes to get ‘interesting’ results. There are two cases of interest: (1) the waves do not ‘hit’ the potential barrier and (2) the waves do hit the potential barrier. First, we replace the potential barrier by a large number of steps as in the step-barrier problem in quantum mechanics. Fig. 1 shows one such example of the potential barrier V_+ (eq. 17) which is drawn for $a = 0.5$, $m_p = 0.8$ and $\sigma = 0.8$. In reality we use tens of thousands of steps with suitable variable widths so that the steps become indistinguishable from the actual function. The solution of (17) at n th step can be written as (Davydov 1976),

$$Z_{+,n} = A_n \exp[ik_n \hat{r}_{*,n}] + B_n \exp[-ik_n \hat{r}_{*,n}] \quad (19)$$

when energy of the wave is greater than the height of the potential barrier. The standard junction condition is given as (Davydov 1976),

$$Z_{+,n} = Z_{+,n+1} \quad \text{and} \quad \frac{dZ_+}{d\hat{r}_*}|_n = \frac{dZ_+}{d\hat{r}_*}|_{n+1}. \quad (20)$$

The reflection and transmission co-efficients at n th junction are given by:

$$R_n = \frac{A_{n+1}(k_{n+1} - k_n) + B_{n+1}(k_{n+1} + k_n)}{A_{n+1}(k_{n+1} + k_n) + B_{n+1}(k_{n+1} - k_n)}; \quad T_n = 1 - R_n \quad (21)$$

At each of the n steps these conditions were used to connect solutions at successive steps. Here, k is the wave number ($k = \sqrt{\sigma^2 - V_{\pm}}$) of the wave and k_n is its value at n th step. We use the ‘no-reflection’ inner boundary condition: $R \rightarrow 0$ at $\hat{r}_* \rightarrow -\infty$.

For the cases where waves hit on the potential barrier, inside the barrier (where $\sigma^2 < V_+$)

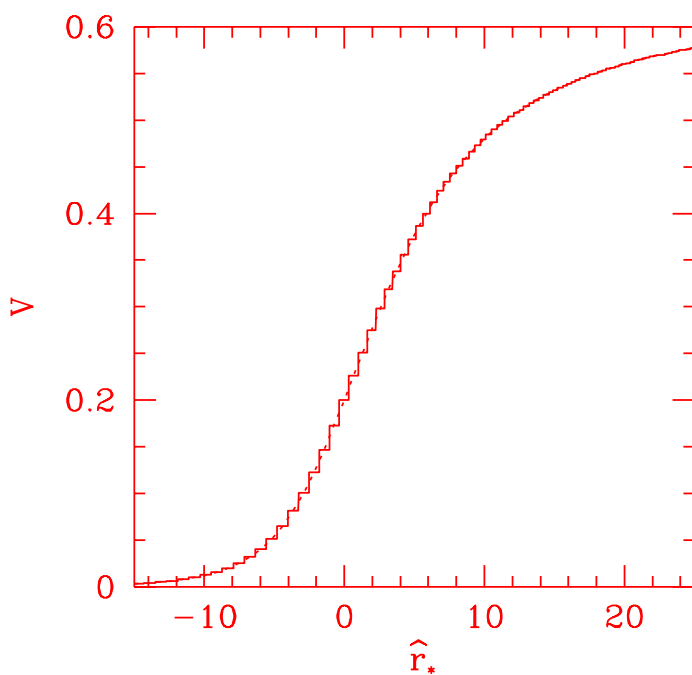


Fig. 1 : Behaviour of V_+ (smooth solid curve) for $a = 0.5$, $m_p = 0.8$, $\sigma = 0.8$. This is approximated as a collection of steps. In reality tens of thousand steps were used with varying step size which mimic the potential with arbitrary accuracy.

we use the wave function of the form

$$Z_{+,n} = A_n \exp[-\alpha_n \hat{r}_{*,n}] + B_n \exp[\alpha_n \hat{r}_{*,n}] \quad (22)$$

where, $\alpha_n = \sqrt{V_{\pm} - \sigma^2}$, as in usual quantum mechanics.

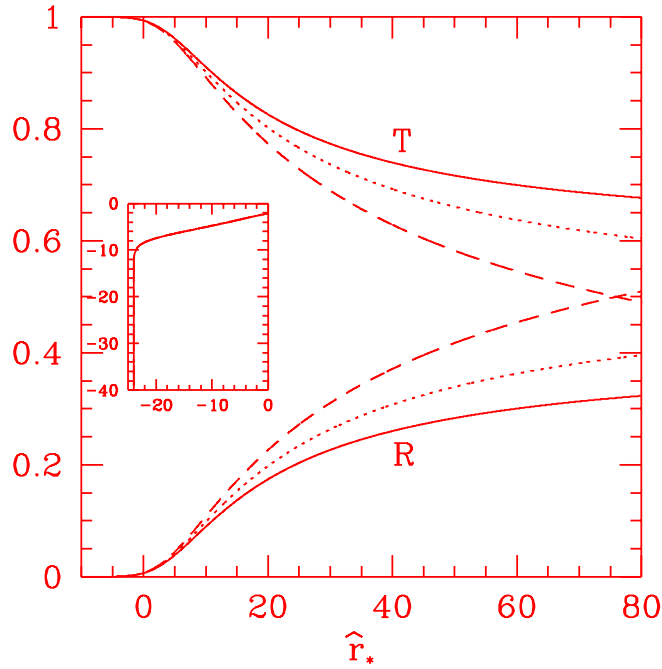


Fig. 2a: Reflection (R) and transmission (T) coefficients of waves with varying mass as functions of \hat{r}_* . $m_p = 0.78$ (solid), $m_p = 0.79$ (dotted) and $m_p = 0.80$ (long-dashed) are used. Other parameters are $a = 0.5$ and $\sigma = 0.8$. Inset shows R in logarithmic scale which falls off exponentially just outside the horizon.

3 EXAMPLES OF SOLUTIONS

Fig. 2a shows three solutions [amplitudes of $\text{Re}(Z_+)$] for parameters: $a = 0.5$, $\sigma = 0.8$ and $m_p = 0.78$, 0.79 , and 0.80 respectively in solid, dotted and long-dashed curves. The energy σ^2 is always higher compared to the height of the potential barrier (Fig. 1) and therefore the particles do not ‘hit’ the barrier. k goes up and therefore the wavelength goes down

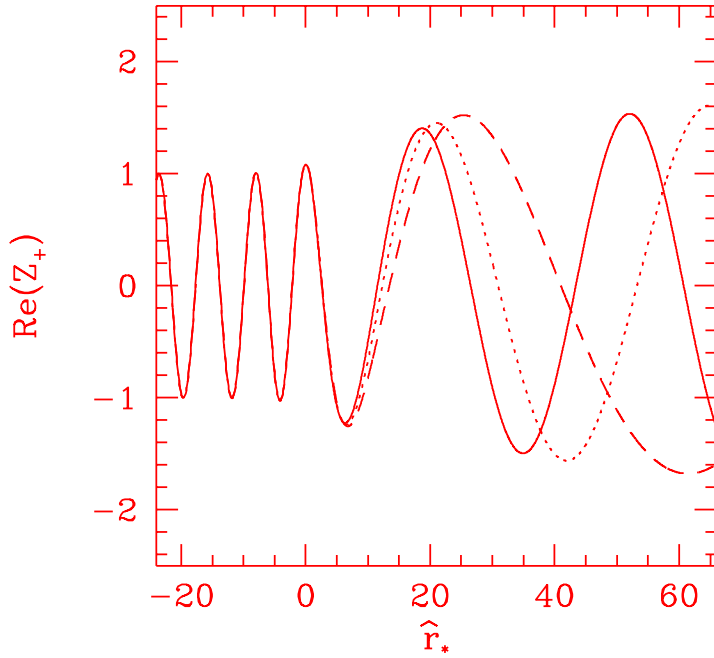


Fig. 2b: Amplitude of $\text{Re}(Z_+)$ of waves with varying mass as functions of \hat{r}_* . $m_p = 0.78$ (solid), $m_p = 0.79$ (dotted) and $m_p = 0.80$ (long-dashed) are used. Other parameters are $a = 0.5$ and $\sigma = 0.8$.

monotonically as the wave approaches a black hole. It is to be noted that though ours is apparently a ‘crude’ method, it has flexibility and is capable of presenting insight into the problem, surpassing any other method such as ODE solver packages. This is because one can choose (a) variable steps depending on steepness of the potential to ensure uniform accuracy, and at the same time (b) virtually infinite number of steps to follow the potential

as closely as possible. For instance, in the inset, we show R in logarithmic scale very close to the horizon. All the three curves merge, indicating that the solutions are independent of the mass of the particle and a closer inspection shows that here, the slope of the curve depends only on σ . The exponential dependence of R_n close to the horizon becomes obvious. Asymptotically, $V_{\pm} = m_p^2$ (eq. 17), thus, as m_p goes down, the wavelength goes down. In Fig. 2b, we present the instantaneous values of the reflection R and transmission T coefficients (i.e., R_n and T_n of eq. 21) for the same three cases. As the particle mass is decreased, k goes up and corresponding R goes down consistent with the limit that as $k \rightarrow \infty$, there would be no reflection at all as in a quantum mechanical problem.

Figs. 3(a-b) compare a few solutions where the incoming particles ‘hit’ the potential barrier. We choose, $a = 0.95$, $\sigma = 0.168$ and mass of the particle $m_p = 0.16, 0.164, 0.168$ respectively in solid, dotted and long-dashed curves. Inside the barrier, the wave decays before coming back to a sinusoidal behaviour, before entering into a black hole. In Fig. 3b, we plotted the potential (shifted by 2.05 along vertical axis for clarity). Here too, the reflection coefficient goes down as k goes up consistent with the classical result that as the barrier height goes up more and more, reflection is taking place strongly. Note however, that the reflection is close to a hundred percent. Tunneling causes only a few percent to be lost into the black hole.

Figs. 4(a-b) show the nature of the complete wave function when both the radial and the angular solutions (Chakrabarti 1984) are included. Fig. 4a shows contours of constant amplitude of the wave ($R_{-1/2}S_{-1/2}$) in the meridional plane – X is along radial direction in the equatorial plane and Y is along the vertical direction. The parameters are $a = 0.5$, $m_p = 0.8$ and $\sigma = 0.8$. Some levels are marked. Two successive contours have amplitude difference of 0.1. In Fig. 4b a three-dimensional nature of the complete solution is given. Both of these figures clearly show how the wavelength varies with distance. Amplitude of the spherical wave coming from a large distance also gets weaker along the vertical axis and the wave is forced to fall generally along the equatorial plane, possibly due to the dragging of the inertial frame.

4 CONCLUSION

Scatterings of massive, spin-half particles from a spinning black hole has been studied with particular emphasis to the nature of the radial wave functions and the reflection and trans-

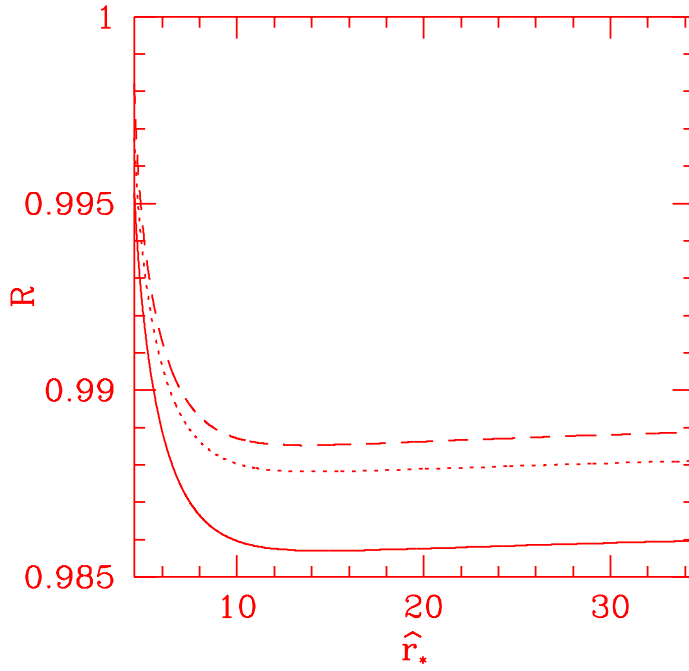


Fig. 3a: Reflection (R) coefficient of waves with varying mass as functions of \hat{r}_* . $m_p = 0.16$ (solid), $m_p = 0.164$ (dotted) and $m_p = 0.168$ (long-dashed) are used. Other parameters are $a = 0.95$ and $\sigma = 0.168$.

mission coefficients. Well known quantum mechanical step-potential approach is used but we applied it successfully to a complex problem of barrier penetration in a spacetime around a spinning black hole. Among significant observations, we find that the wave function and R , and T behave similarly close to the horizon independent of the initial parameter, such as the particle mass m_p . Particles of different mass scatter off to a large distance completely differ-

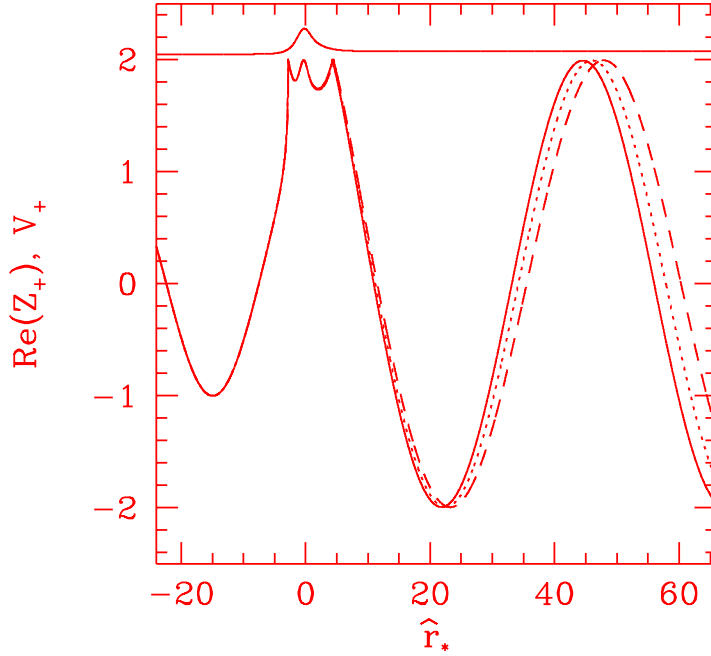


Fig. 3b: Amplitude of $\text{Re}(Z_+)$ of waves with varying mass as functions of \hat{r}_* . $m_p = 0.16$ (solid), $m_p = 0.164$ (dotted) and $m_p = 0.168$ (long-dashed) are used. Nature of potential with $m_p = 0.168$ is drawn shifting vertically by 2.05 unit for clarity. Other parameters are $a = 0.95$ and $\sigma = 0.168$.

ently, thus giving an impression that a black hole could be treated as a mass spectrograph! When the energy of the particle becomes higher compared to the rest mass, the reflection coefficient diminishes as it should it. Similar to a barrier penetration problem, the reflection coefficient becomes close to a hundred percent when the wave hits the potential barrier. Another significant observation is that the reflection and transmission coefficients are func-

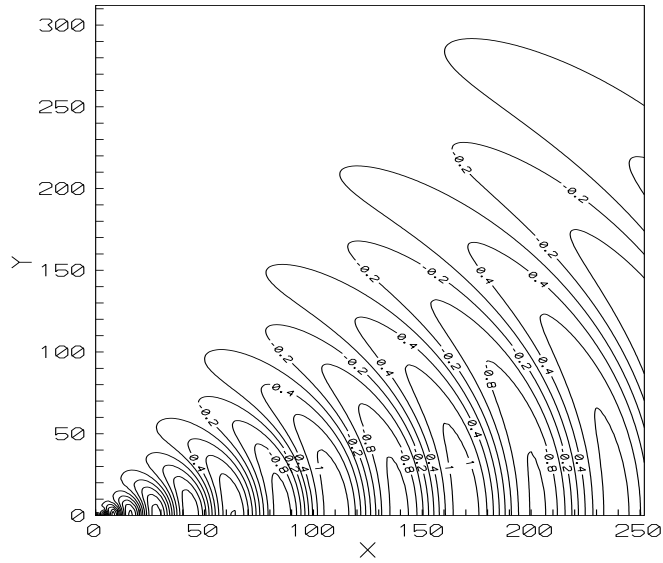


Fig. 4a: Contours of constant amplitude are plotted in the meridional plane around a black hole. Radial direction on equatorial plane is along X axis and the vertical direction and along Y . Both radial and theta solutions have been combined. Parameters are $a = 0.5$, $m_p = 0.8$ and $\sigma = 0.8$.

tions of the radial coordinates. This is understood easily because of the very nature of the potential barrier which is strongly space dependent which we approximate as a collection of steps. Combining with the solution of theta-equation, we find that the wave-amplitude vanishes close to the vertical axis, possibly due to the frame-dragging effects.

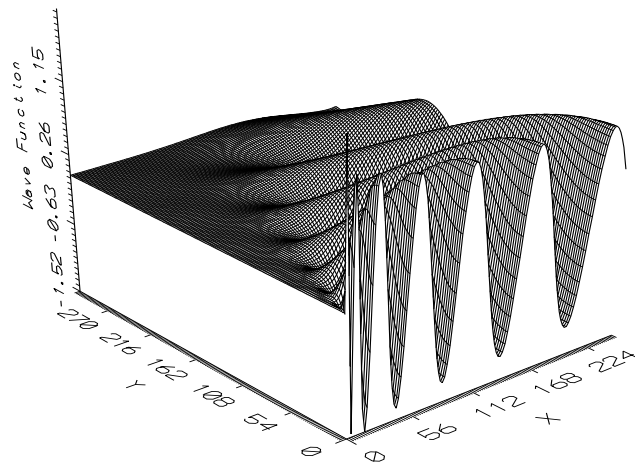


Fig. 4b: Three dimensional view of $R_{-1/2}S_{-1/2}$ are plotted in the meridional plane around a black hole. Both radial and theta solutions have been combined. Parameters are $a = 0.5$, $m_p = 0.8$ and $\sigma = 0.8$.

REFERENCES

- Chandrasekhar 1976, Proc. R. Soc. Lond. A, 349, 571
 Chakrabarti, S.K. 1984, Proc. R. Soc. Lond. A, 391, 27
 Goldberg, J.N., Macfarlane, A.J., Newman, E.T., Rohrlich, F. & Sudarsan, E.C.G. 1967, J. Math. Phys., 8, 2155
 Breure, R.A., Ryan, M.P. Jr. & Waller, S 1982, Proc. R. Soc. Lond. A, 358, 71
 Chandrasekhar, S. 1983, in *The Mathematical Theory Of Black Holes* (London: Clarendon Press).
 Davydov, A.S. 1976 (Second Ed.) in *Quantum Mechanics* (Oxford, New York: Pergamon Press).